Revealing the Mechanism of the Low-Energy Electron Yield Enhancement from Sensitizing Nanoparticles

Alexey V. Verkhovtsev,[1,2,*] Andrei V. Korol,[1,3,†] and Andrey V. Solov'yov[1,2,‡]

[1]*MBN Research Center, Altenhöferallee 3, 60438 Frankfurt am Main, Germany*
[2]*A.F. Ioffe Physical-Technical Institute, Politekhnicheskaya ul. 26, 194021 St. Petersburg, Russia*
[3]*Department of Physics, St. Petersburg State Maritime Technical University, Leninskii Prospekt 101, 198262 St. Petersburg, Russia*

We provide a physical explanation for the enhancement of the low-energy electron production by sensitizing nanoparticles due to irradiation by fast ions. It is demonstrated that a significant increase in the number of emitted electrons arises from the collective electron excitations in the nanoparticle. We predict a new mechanism of the yield enhancement due to the plasmon excitations and quantitatively estimate its contribution to the electron production. Revealing the nanoscale mechanism of the electron yield enhancement, we provide an efficient tool for evaluating the yield of the emitted electron from various sensitizers. It is shown that the number of low-energy electrons generated by the gold and platinum nanoparticles of a given size exceeds that produced by the equivalent volume of water and by other metallic (e.g., gadolinium) nanoparticles by an order of magnitude. This observation emphasizes the sensitization effect of the noble-metal nanoparticles and endorses their application in novel technologies of cancer therapy with ionizing radiation.

PACS numbers: 36.40.Gk, 31.15.ee, 79.20.-m, 87.53.-j

Radiotherapy is now one of the frequently used methods to treat cancer, which is currently a major health concern. However, it has side effects induced by the radiation in the surrounding healthy tissues. One of the promising modern treatment techniques is ion-beam cancer therapy [1–3]. It allows one to deliver a higher dose to the target region, as compared to conventional photon therapy, and also to minimize the exposure of healthy tissue to radiation [1]. Approaches that enhance radiosensitivity within tumors relative to normal tissues have the potential to become advantageous radiotherapies. A search for such approaches is within the scope of several ongoing multidisciplinary projects [4,5].

Metal nanoparticles (NPs) were recently proposed to act as sensitizers in cancer treatments with ionizing radiation [6–8]. The injection of such nanoagents into a tumor can increase the relative biological effectiveness of ionizing radiation, which is defined as the ratio of the dose delivered by photons to that by a different radiation modality, leading to the same biological effects, such as the probability of an irradiated cell death. In recent years, the application of gold NPs acting as dose enhancers, in combination with photons, revealed an increase of cancer cell killing [9–11], while an advantage of using NPs in ion-beam cancer therapy is still to be thoroughly substantiated.

It is currently acknowledged [3,12–14] that a substantial portion of biodamage by incident ions is related to the secondary electrons and free radicals produced due to ionization of the medium by the projectiles. References [15–17] have explored the possibility of low-energy electrons (LEEs), having the kinetic energy from a few eV to several tens of eV, to be important agents of biodamage.

In this Letter, we reveal the physical mechanism of enhancement of the LEE production by sensitizing (noble metal, in particular) NPs. We demonstrate that a significant increase in the number of emitted electrons due to irradiation by fast ions comes from the two distinct types of collective electron excitations. We predict that the yield of the 1–10 eV electrons is strongly enhanced due to the decay of plasmon-type excitations of delocalized valence electrons in metal NPs. More specifically, the leading mechanism of the electron production is associated with the *surface* plasmon, whose contribution to the electron yield exceeds by an order of magnitude that of the volume plasmon, considered in the recent Monte Carlo simulation [18]. For higher electron energies (of about 10–30 eV), the dominating contribution to the electron yield arises from the atomic giant resonances associated with the collective excitation of d electrons in individual atoms in a NP. As a result of these effects, the number of LEEs generated by the noble-metal NP of a given size exceeds that produced by the equivalent volume of water by an order of magnitude. On the basis of the physical understanding of the processes involved, we provide an efficient tool for a quantitative estimate of the yield of emitted electrons from sensitizing NPs.

Studying the electron production by a NP irradiated by ions, we account for the two collective electron effects, namely, excitation of delocalized electrons in a NP (plasmons) and that of d electrons in individual atoms (atomic giant resonances). These phenomena occur in various processes of interaction of ionizing radiation with matter. In particular, dipole collective excitations result in the formation of prominent resonances in the photoabsorption spectra of atomic clusters and nanoparticles [19,20], while
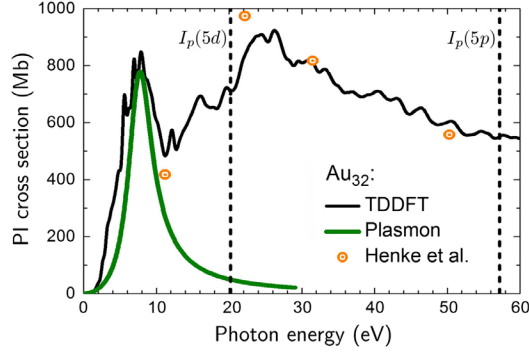
FIG. 1 (color online). Photoabsorption cross section of the Au_{32} cluster calculated within TDDFT (thin curve). Thick curve represents the contribution of the plasmon-type excitations. Symbols represent the data for atomic gold [45], multiplied by the number of atoms in the cluster. Vertical lines mark the $5d$ and $5p$ ionization thresholds in the atom of gold.

the impact ionization cross sections also comprise the contributions of higher multipole terms [21].

We consider noble-metal (gold, platinum, and silver) and other metallic (gadolinium) NPs, which are of interest [6–10] in the application in cancer treatments. As a starting point, we have calculated the photoabsorption spectra of several three-dimensional (3D) gold clusters made of 18–42 atoms. The calculations within the time-dependent density-functional theory (TDDFT) framework [22,23] were performed using the QUANTUM ESPRESSO package [24,25]. A technical description of the calculations is presented in the Supplemental Material [26]. As a case study, Fig. 1 presents the TDDFT-based spectrum of the Au_{32} cluster in the photon energy range up to 60 eV (thin black curve). The spectrum is characterized by a low-energy peak located below 10 eV and by a broad feature with a maximum at about 25 eV. The results of the calculation are compared to the x-ray absorption data for atomic gold [45], multiplied by the number of atoms in the cluster.

Our analysis has revealed that the high-energy feature is the atomic giant resonance formed due to the excitation of electrons in the $5d$ atomic shell. The integration of the oscillator strength from 20.2 eV (ionization threshold of the $5d$ shell in the atom of gold) up to 57.2 eV (the $5p$ shell ionization threshold [45]), indicates that about eight localized d electrons contribute to the excitation of the $5d$ shell forming the broad peak in the spectrum. The low-energy peak is due to the plasmon-type excitation, which involves some fraction of s and d electrons delocalized over the whole cluster. The delocalization comes from a partial hybridization of the $6s$ and $5d$ atomic shells. The integration of the oscillator strength up to 11.2 eV (energy at which the first dip after the resonance peak is observed in the TDDFT spectrum) reveals that about 1.5 electrons from each atom contribute to the collective plasmon-type excitation, indicating delocalization of some fraction of d electrons [44]. Thus, the total photoabsorption spectrum of a gold NP in the energy region up to 60 eV approximately is equal to

the sum of the plasmon contribution and that of the $5d$ electron excitations in individual atoms, $\sigma_\gamma \approx \sigma_{pl} + \sigma_{5d}$.

Similar to the photoionization, the two distinct types of collective electron excitations appear in the process of impact ionization. We use the methodology allowing us to analyze the role of these contributions to the electron production by sensitizing NPs separately. The single differential inelastic scattering cross section of a fast projectile in collision with a NP is given by a general formula (we use the atomic system of units, $m_e = |e| = \hbar = 1$)

$$\frac{d\sigma}{d\Delta\varepsilon} = \frac{2\pi}{p_1 p_2} \int_{q_{min}}^{q_{max}} q dq \frac{d^2\sigma}{d\Delta\varepsilon d\Omega_{\mathbf{p}_2}} \approx \frac{d\sigma_{pl}}{d\Delta\varepsilon} + \frac{d\sigma_{at}}{d\Delta\varepsilon}, \quad (1)$$

where $\Delta\varepsilon = \varepsilon_1 - \varepsilon_2$ is the energy loss of the incident projectile of energy ε_1, $\mathbf{p}_1$ and $\mathbf{p}_2$ are the initial and the final momenta of the projectile, $\Omega_{\mathbf{p}_2}$ is its solid angle, and $\mathbf{q} = \mathbf{p}_1 - \mathbf{p}_2$ is the transferred momentum. The cross sections $d\sigma_{pl}$ and $d\sigma_{at}$ denote the contributions of the plasmon and individual atomic excitations, respectively.

The contribution of the plasmon excitations to the ionization cross section is described by means of the plasmon resonance approximation (PRA) [19,43,46,47], which postulates that the collective excitations dominate the cross section in the vicinity of the plasmon resonance. During the past years, the PRA was successfully applied to explain the resonantlike structures in photoionization spectra [41,46] and differential inelastic scattering cross sections [47–49] of metal clusters and carbon fullerenes by the photon and electron impact. Within the PRA, the double differential cross section $d^2\sigma/d\Delta\varepsilon d\Omega_{\mathbf{p}_2}$ for a spherical NP is defined as a sum of the surface (s) and the volume (v) plasmon terms, which are constructed as a sum over different multipole contributions corresponding to different values of the angular momentum l [47],

$$\frac{d^2\sigma^{(s)}}{d\Delta\varepsilon d\Omega_{\mathbf{p}_2}} \propto \sum_l \frac{\omega_l^{(s)2}\Gamma_l^{(s)}}{(\omega^2 - \omega_l^{(s)2})^2 + \omega^2\Gamma_l^{(s)2}},$$

$$\frac{d^2\sigma^{(v)}}{d\Delta\varepsilon d\Omega_{\mathbf{p}_2}} \propto \sum_l \frac{\omega_p^2\Gamma_l^{(v)}}{(\omega^2 - \omega_p^2)^2 + \omega^2\Gamma_l^{(v)2}}. \quad (2)$$

Here, $\omega_l^{(s)} = \sqrt{l/(2l+1)}\,\omega_p$ is the frequency of the surface plasmon of the multipolarity l, and $\omega_p = \sqrt{4\pi\rho_0} = \sqrt{3N_e/R^3}$ is the volume plasmon frequency associated with the density ρ_0 of N_e delocalized electrons. The quantities $\Gamma_l^{(i)}$ $(i = s, v)$ are the plasmon widths. In the analysis, we accounted for the dipole $(l = 1)$, quadrupole $(l = 2)$, and octupole $(l = 3)$ terms. Excitations with larger l values have a single-particle rather than a collective nature [47], thus, not contributing to the plasmon formation. Explicit expressions for the cross sections (2), obtained within the first Born approximation, are presented in Ref. [43]. This approach is applicable for the collision of a nanoparticle with a fast heavy projectile.

The PRA relies on a few parameters, which include the oscillator strength of the plasmon excitation, position of the

peak, and its width. In the dipole case, these were validated by fitting the TDDFT-based spectra of several 3D gold clusters to those calculated within the model approach. We assumed that 1.5 electrons from each gold atom contribute to the plasmon excitation. This value, along with the dipole plasmon width $\Gamma_1^{(s)} = 4.0$ eV $\approx 0.6\omega_1^{(s)}$, was used to reproduce the low-energy peak in the photoabsorption spectra of gold clusters by means of the PRA scheme (see the solid green curve in Fig. 1). The similar ratio of the plasmon resonance width to its frequency was assumed for higher multipole terms of the surface plasmon [50] and for the volume plasmon as well, $\Gamma_l^{(s)}/\omega_l^{(s)} = \Gamma_l^{(v)}/\omega_p = 0.6$.

Atomic d electrons in noble metals play a dominant role at higher excitation energies, from approximately 20 to 60 eV (see Fig. 1 for the case of gold). For distant collisions, i.e., when the impact parameter exceeds the radius R of the atomic subshell, the ionization spectra are dominated by the dipole term [52]. Comparing the cross sections of photoionization σ_γ and the dipole term of inelastic scattering $d\sigma_{at}/d\Delta\varepsilon$, calculated in the Born approximation, one derives the following expression:

$$\frac{d\sigma_{at}}{d\Delta\varepsilon} = \frac{2c}{\pi\omega v_1^2}\sigma_\gamma \ln\left(\frac{v_1}{\omega R}\right), \qquad (3)$$

where $\omega = \varepsilon_1 - \varepsilon_2$ is the energy transfer, and v_1 is the projectile velocity. Equation (3), obtained within the so-called "logarithmic approximation", assumes that the main contribution to the cross section $d\sigma_{at}/d\Delta\varepsilon$ comes from the region of large distances $R < r < v_1/\omega$. This relation has the logarithmic accuracy that implies that the logarithmic term dominates the cross section while all nonlogarithmic terms are neglected [53]. For the studied noble-metal atoms, we assumed $\omega \approx 1$ a.u., which corresponds to the maximum of the $5d(4d)$ giant resonance in gold and platinum (silver) [45], $v_1 \approx 6.3$ a.u. for a 1 MeV proton, and the electron shell radii $R_{5d}(\mathrm{Au}, \mathrm{Pt}) \approx R_{4d}(\mathrm{Ag}) \approx 2$ a.u.. Note that the interaction of the incident projectile with the NP leads to the formation of the giant resonance not in all atoms of the system but only in those located within the impact parameter interval from $r_{min} \simeq R_{5d}(R_{4d})$ to $r_{max} \simeq v_1/\omega$. This estimate reveals that the resonance is excited in approximately one third of the atoms. A similar estimate was also made for a Gd atom. Contrary to the noble metals, the Gd atom has a single electron in the $5d$ shell. Thus, there is no atomic giant resonance in the ionization spectrum of Gd in the 20–60 eV range, and the spectrum is characterized by a narrow peak at $\omega \approx 1.2$ a.u., formed due to ionization of the $5p$ shell.

To quantify the production of secondary electrons in collision with the nanoparticles, the cross section $d\sigma/d\Delta\varepsilon$, Eq. (1), is redefined as a function of the kinetic energy E of the electrons $E = \Delta\varepsilon - I_p$, where I_p is the ionization threshold of the system. The cross section $d\sigma/dE$ can be related to the probability to produce N electrons with kinetic energy within the interval dE, emitted from a segment dx of the trajectory, via [3]
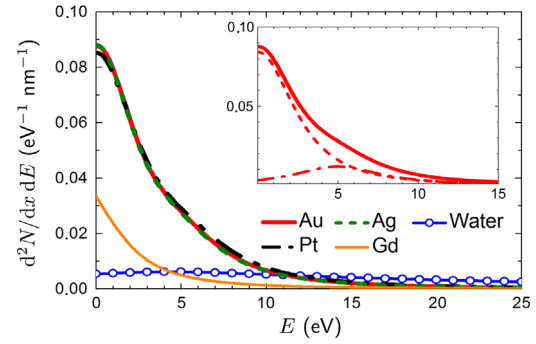

FIG. 2 (color online). Number of electrons per unit length per unit energy produced via the plasmon excitations in the Au, Pt, Ag, and Gd NPs irradiated by a 1 MeV proton. Open circles represent the number of electrons generated from the equivalent volume of water [54]. Inset: contributions of the surface (dashed line) and the volume (dash-dotted line) plasmons to the electron yield from the AuNP.

$$\frac{d^2N(E)}{dx\,dE} = n\frac{d\sigma}{dE}, \qquad (4)$$

where n is the atomic density of the target.

Figure 2 presents the number of electrons per unit length per unit energy produced via the "plasmon excitation" mechanism by the 1 nm spherical NPs due to 1 MeV proton irradiation. We have also compared the electron production by the NPs and by the equivalent volume of pure water medium [54]. Comparative analysis of the spectra demonstrates that the number of LEEs (with the kinetic energy of about a few eV) produced due to the plasmon excitations in the noble-metal NPs is about 1 order of magnitude higher than that by liquid water. The enhancement of the LEE yield due to the presence of sensitizing NPs may increase the probability of the tumor cell destruction due to the higher number of double- and multiple-strand breaks of the DNA. Thus, the plasmon decay in the nanoparticles, embedded in a biological medium, represents an important channel for the production of low-energy secondary electrons in the medium.

It was demonstrated recently [8] that tumor-targeted Gd-based NPs amplify cell death under ion irradiation and also enhance the number of single- and double-strand breaks in plasmid DNA. However, it was noted that the effect of GdNPs is less pronounced than that of platinum-based compounds. This result generally corresponds to our conclusions that the electron yield from a GdNP exceeds the electron production from pure water medium but is lower than that from noble-metal NPs.

The low electron yield from the GdNP, as compared to the noble-metal targets, is explained by the density effects (the atomic density of Gd is about 2 times smaller than that of the studied noble metals) as well as by the lower plasmon frequency. The maximum of the plasmon resonance peak in the GdNP (4.1 eV) is located below the ionization potential of the system (~ 5.0 eV) [55]. In the case of noble-metal NPs, the plasmon peak maxima are in the range between 5.5 and 6.0 eV, being in the vicinity of the ionization thresholds.

Therefore, the plasmon decay in noble-metal NPs results in more intense electron emission as compared to that of GdNP. In the latter case, the plasmon will mostly decay into the single-electron excitations, which can lead to the vibration of the ionic core as a result of the electron-phonon coupling [56].

The inset of Fig. 2 demonstrates that the *surface* plasmon (dashed curve) gives the dominant contribution to the electron production by the metallic NP (as a case study, we consider gold) exceeding that of the *volume* plasmon (dash-dotted curve) by an order of magnitude. The significance of the plasmon excitations in the process of electron production by sensitizing NPs, revealed in this Letter, repudiates the statement made in Ref. [18] on the negligible role of the plasmon excitations in forming the spectrum of emitted electrons. Let us stress that only the volume plasmon excitation was accounted for in the cited paper. Our more extended analysis [57] reveals that the plasmon excitations play a prominent role in the production of LEEs from gold NPs of about 1–5 nm in diameter. This size range corresponds to the size of noble-metal and Gd-based NPs studied recently in relation to the radiotherapies with charged ions [6,8].

To estimate the total number of electrons produced due to the collective excitations in the NPs, we have also accounted for the contribution of excitations in individual atoms. Figure 3 demonstrates the relative enhancement of the electron yield from the considered nanoparticles as compared to that of pure water. This quantity was obtained by summing up the contribution of the plasmons and individual atomic excitations. The dashed lines present the contribution of the atomic giant resonances ($5d$ in Au and Pt, and $4d$ in Ag) as well as the total $5p + 5d$ contribution in Gd, estimated using Eq. (3). Making this estimate, we have assumed that the ionization cross sections are dominated by the dipole excitation. Contributions of quadrupole and higher multipole terms will lead to an increase in the number of emitted electrons, but their relative contribution will be not as large as that from the dipole excitation. The solid line is the sum of the excitations in individual atoms and the plasmons. The significant yield enhancement arises in those nanoparticles whose constituent atoms possess the giant resonance, contrary to the case of gadolinium, which has a single $5d$ electron. Accounting for the plasmon contribution leads to a significant increase of the 1–5 eV electron yield. Because of the collective electron excitations arising in these systems, the gold and platinum NPs can thus produce a much larger (of about an order of magnitude) number of LEEs compared to the equivalent volume of a pure water medium. We note that the enhanced production of LEEs will also lead to an increase in the number of free radicals as well as other reactive species, such as hydrogen peroxide H_2O_2, which can travel large distances within the cell [8]. Thus, these species can deliver damaging impacts onto DNA from the radiation-induced damages associated with the presence of NPs in other cell compartments, such as lysosomes [58].

To conclude, we have analyzed the electron production by sensitizing metallic nanoparticles due to irradiation by
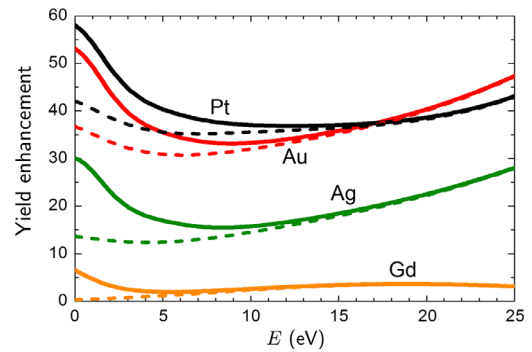

FIG. 3 (color online). Yield enhancement from 1 nm metallic NPs. Dashed lines show the contribution of individual atomic excitations. Solid lines show the resulting contribution with an account of the plasmons.

fast ions and revealed the physical mechanism of low-energy electron yield enhancement. It has been shown that the significant increase in the number of emitted electrons arises from the two distinct types of collective electron excitations formed in nanoparticles. The yield enhancement is caused by the plasmons, excited in a whole nanoparticle, and by the excitation of d electrons in individual atoms that results in the formation of giant atomic resonances. The plasmon excitation mechanism leads a significant additional increase of the electron yield enhancement from the noble-metal nanoparticles compared to that of water. Thus, the damping of the plasmons excited in the metal nanoparticles represents an important mechanism of the low-energy electron generation.

In this Letter, we have introduced a general methodology which can be applied for other nanoscale systems proposed as sensitizers in cancer therapy. Particularly, it can be applied to study more complex types of sensitizers, for instance, core-shell nanoparticles, where the collective electron excitations will arise in both parts of the system. A proper choice of the constituents will allow one to tune the position of the resonance peaks in the ionization spectra of such systems and, subsequently, to cover a broader kinetic energy spectrum of electrons emitted from these nanoparticles. The utilized methodology can also be adopted for different projectiles, e.g., carbon ions, which are the most clinically used projectiles, besides protons.

*verkhovtsev@mail.ioffe.ru
†korol@th.physik.uni-frankfurt.de
‡solovyov@mbnresearch.com

[1] D. Schardt, T. Elsässer, and D. Schulz-Ertner, Heavy-ion tumor therapy: Physical and radiobiological benefits, Rev. Mod. Phys. **82**, 383 (2010).

[2] M. Durante and J. S. Loeffler, Charged particles in radiation oncology , Nat. Rev. Clin. Oncol. **7**, 37 (2010).

[3] E. Surdutovich and A. V. Solov'yov, Multiscale approach to the physics of radiation damage with ions, Eur. Phys. J. D **68**, 353 (2014).

[4] European COST Action Nanoscale Insights into Ion-Beam Cancer Therapy (Nano-IBCT), http://www.cost.eu/domains_actions/mpns/Actions/nano-ibct/.

[5] FP7 Initial Training Network Project Advanced Radio-therapy, Generated by Exploiting Nanoprocesses and Technologies (ARGENT), http://www.itn-argent.eu.

[6] E. Porcel, S. Liehn, H. Remita, N. Usami, K. Kobayashi, Y. Furusawa, C. Le Sech, and S. Lacombe, Platinum nano-particles: A promising material for future cancer therapy?, Nanotechnology **21**, 085103 (2010).

[7] P. Liu, Z. Huang, Z. Chen, R. Xu, H. Wu, F. Zang, C. Wang, and N. Gu, Silver nanoparticles: A novel radiation sensitizer for glioma?, Nanoscale **5**, 11829 (2013).

[8] E. Porcel et al., Gadolinium-based nanoparticles to improve the hadrontherapy performances, Nanomed. Nanotech. Biol. Med. **10**, 1601 (2014).

[9] S. J. McMahon et al., Biological consequences of nanoscale energy deposition near irradiated heavy atom nanoparticles, Sci. Rep. **1**, 18 (2011).

[10] S. Jain et al., Cell-specific radiosensitization by gold nano-particles at megavoltage radiation energies, Int. J. Radiat. Oncol. Biol. Phys. **79**, 531 (2011).

[11] J. J. Hainfeld, D. N. Slatkin, and H. M. Smilowitz, The use of gold nanoparticles to enhance radiotherapy in mice, Phys. Med. Biol. **49**, N309 (2004).

[12] B. D. Michael and P. O'Neill, Molecular biology. A sting in the tail of electron tracks, Science **287**, 1603 (2000).

[13] Radiation Damage in Biomolecular Systems, edited by G. Garcia Gomez-Tejedor and M. C. Fuss (Springer Science+Business Media B.V., Dordrecht, The Netherlands, 2012).

[14] A. V. Solov'yov, E. Surdutovich, E. Scifoni, I. Mishustin, and W. Greiner, Physics of ion beam cancer therapy: A multiscale approach, Phys. Rev. E **79**, 011909 (2009).

[15] B. Boudaïffa, P. Cloutier, D. Hunting, M. A. Huels, and L. Sanche, Resonant formation of DNA strand breaks by low-energy (3 to 20 eV) electrons, Science **287**, 1658 (2000).

[16] M. A. Huels, B. Boudaiffa, P. Cloutier, D. Hunting, and L. Sanche, Single, double, and multiple double strand breaks induced in DNA by 3-100 eV electrons, J. Am. Chem. Soc. **125**, 4467 (2003).

[17] M. Toulemonde, E. Surdutovich, and A. V. Solov'yov, Temperature and pressure spikes in ion-beam cancer therapy, Phys. Rev. E **80**, 031913 (2009).

[18] C. Wälzlein, E. Scifoni, M. Krämer, and M. Durante, Simulations of dose enhancement for heavy atom nano-particles irradiated by protons, Phys. Med. Biol. **59**, 1441 (2014).

[19] U. Kreibig and M. Vollmer, Optical Properties of Metal Clusters (Springer-Verlag, Berlin-Heidelberg, 1995).

[20] P. M. Dinh, P.-G. Reinhard, and E. Suraud, An Introduction to Cluster Science (Wiley, New York, 2013).

[21] L. G. Gerchikov, A. N. Ipatov, and A. V. Solov'yov, Many-body treatment of electron inelastic scattering on metal clusters, J. Phys. B **30**, 5939 (1997).

[22] E. Runge and E. K. U. Gross, Density-Functional Theory for Time-Dependent Systems, Phys. Rev. Lett. **52**, 997 (1984).

[23] B. Walker, A. M. Saitta, R. Gebauer, and S. Baroni, Efficient Approach to Time-Dependent Density-Functional Perturbation Theory for Optical Spectroscopy, Phys. Rev. Lett. **96**, 113001 (2006).

[24] P. Giannozzi et al., QUANTUM ESPRESSO: A modular and open-source software project for quantum simulations of materials, J. Phys. Condens. Matter **21**, 395502 (2009).

[25] O. B. Malcioğlu, R. Gebauer, D. Rocca, and S. Baroni, TurboTDDFT - A code for the simulation of molecular spectra using the Liouville-Lanczos approach to time-dependent density-functional perturbation theory , Comput. Phys. Commun. **182**, 1744 (2011).

[26] See the Supplemental Material at http://link.aps.org/supplemental/10.1103/PhysRevLett.114.063401, which includes Refs. [27–44] for the analysis of the nature of the valence states in the Au_{32} cluster and for technical details of the DFT/TDDFT calculations.

[27] U. Fano, A common mechanism of collective phenomena, Rev. Mod. Phys. **64**, 313 (1992).

[28] S. Malola, L. Lehtovaara, J. Enkovaara, and H. Häkkinen, Birth of the localized surface plasmon resonance in mono-layer-protected gold nanoclusters, ACS Nano **7**, 10263 (2013).

[29] N. Durante, A. Fortunelli, M. Broyer, and M. Stener, Optical properties of Au nanoclusters from TD-DFT calculations, J. Phys. Chem. C **115**, 6277 (2011).

[30] R. Philip, P. Chantharasupawong, H. Qian, R. Jin, and J. Thomas, Evolution of nonlinear optical properties: From gold atomic clusters to plasmonic nanocrystals, Nano Lett. **12**, 4661 (2012).

[31] M. Stener, A. Nardelli, R. De Francesco, and G. Fronzoni, Optical excitations of gold nanoparticles: A quantum chemical scalar relativistic time dependent density functional study, J. Phys. Chem. C **111**, 11862 (2007).

[32] M. P. Johansson, D. Sundholm, and J. Vaara, Au_{32}: A 24-carat golden fullerene, Angew. Chem., Int. Ed. Engl. **43**, 2678 (2004).

[33] X. Gu, M. Ji, S. H. Wei, and X. G. Gong, Au_N clusters ($N = 32, 33, 34, 35$): cagelike structures of pure metal atoms, Phys. Rev. B **70**, 205401 (2004).

[34] M. J. Frisch et al., Gaussian 09 Revision A.1, Gaussian Inc., Wallingford, CT, 2009.

[35] W. J. Stevens, M. Krauss, H. Basch, and P. G. Jasien, Relativistic compact effective potentials and efficient, shared-exponent basis-sets for the third-, fourth-, and fifth-row atoms, Can. J. Chem. **70**, 612 (1992).

[36] J. P. Perdew, K. Burke, and M. Ernzerhof, Generalized Gradient Approximation Made Simple, Phys. Rev. Lett. **77**, 3865 (1996).

[37] M. S. Dresselhaus, G. Dresselhaus, and A. Jorio, Group Theory: Application to the Physics of Condensed Matter (Springer, New York, 2010).

[38] C. M. Aikens, S. Li, and G. C. Schatz, From discrete electronic states to plasmons: TDDFT optical absorption properties of Ag_n ($N = 10, 20, 35, 56, 84, 120$) tetrahedral clusters, J. Phys. Chem. C **112**, 11272 (2008).

[39] B. Walker and R. Gebauer, Ultrasoft pseudopotentials in time-dependent density-functional theory, J. Chem. Phys. **127**, 164106 (2007).

[40] D. Rocca, R. Gebauer, Y. Saad, and S. Baroni, Turbo charging time-dependent density-functional theory with lanczos chains, J. Chem. Phys. **128**, 154105 (2008).

[41] A. V. Verkhovtsev, A. V. Korol, and A. V. Solov'yov, Quantum and classical features of the photoionization spectrum of C_{60}, Phys. Rev. A **88**, 043201 (2013).

[42] D. Vanderbilt, Soft self-consistent pseudopotentials in a generalized eigenvalue formalism , Phys. Rev. B **41**, 7892 (R) (1990).

[43] A. V. Verkhovtsev, A. V. Korol, and A. V. Solov'yov, Formalism of collective excitations in fullerenes, Eur. Phys. J. D **66**, 253 (2012).

[44] E. M. Fernández, J. M. Soler, and L. C. Balbás, Planar and cagelike structures of gold clusters: Density-functional pseudopotential calculations, Phys. Rev. B **73**, 235433 (2006).

[45] B. L. Henke, E. M. Gullikson, and J. C. Davis, X-Ray interactions: Photoabsorption, scattering, transmission, and reflection at $E = 50 - 30,000$ eV, $Z = 1 - 92$, At. Data Nucl. Data Tables **54**, 181 (1993).

[46] J.-P. Connerade and A. V. Solov'yov, Formalism for multi-photon plasmon excitation in jellium clusters, Phys. Rev. A **66**, 013207 (2002).

[47] A. V. Solov'yov, Plasmon excitations in metal clusters and fullerenes, Int. J. Mod. Phys. B **19**, 4143 (2005).

[48] L. G. Gerchikov, P. V. Efimov, V. M. Mikoushkin, and A. V. Solov'yov, Diffraction of Fast Electrons on the Fullerene C_{60} Molecule, Phys. Rev. Lett. **81**, 2707 (1998).

[49] A. V. Verkhovtsev, A. V. Korol, A. V. Solov'yov, P. Bolognesi, A. Ruocco, and L. Avaldi, Interplay of the Volume and Surface Plasmons in the Electron Energy Loss Spectra of C_{60}, J. Phys. B **45**, 141002 (2012).

[50] We estimated $\Gamma_l^{(s)}$ using the relation from Ref. [51], which is similar to the Landau damping of plasmon oscillations in electron gas $\Gamma_l^{(s)} = A v_F / R$, where v_F is the Fermi velocity of delocalized electrons in the NP of radius R, and A is a dimensionless constant of order unity.

[51] C. Yannouleas and R. A. Broglia, Landau damping and wall dissipation in large metal clusters, Ann. Phys. (N.Y.) **217**, 105 (1992).

[52] L. D. Landau and E. M. Lifshitz, *Quantum Mechanics: Non-Relativistic Theory*, 3rd ed., Course of Theoretical Physics Vol. 3 (Butterworth-Heinemann, Oxford, England, 1976).

[53] A. V. Korol and A. V. Solov'yov, *Polarization Bremsstrahlung*, Springer Series on Atomic, Optical, and Plasma Physics Vol. 80 (Springer, New York, 2014).

[54] P. de Vera, R. Garcia-Molina, I. Abril, and A. V. Solov'yov, Semiempirical Model for the Ion Impact Ionization of Complex Biological Media, Phys. Rev. Lett. **110**, 148104 (2013).

[55] H. K. Yuan, H. Chen, C. L. Tian, A. L. Kuang, and J. Z. Wang, Density functional calculations for structural, electronic, and magnetic properties of gadolinium-oxide clusters, J. Chem. Phys. **140**, 154308 (2014).

[56] L. G. Gerchikov, A. N. Ipatov, A. V. Solov'yov, and W. Greiner, Non-adiabatic electron-ion coupling in dynamical jellium model for metal clusters, J. Phys. B **33**, 4905 (2000).

[57] A. V. Verkhovtsev, A. V. Korol, and A. V. Solov'yov, Electron production by sensitizing noble metal nanoparticles irradiated by fast ions, J. Phys. Chem. C (to be published).

[58] L. Štefančíková *et al.*, Cell localisation of gadolinium-based nanoparticles and related radiosensitising efficacy in glioblastoma cells, Cancer Nanotechnol. **5**, 6 (2014).